FLOW CHARACTERISTICS IN TURBULENT SEPARATING AND REATTACHING FLOWS OVER PERMEABLE POROUS WALLS

S. Tominaga, M. Mori, M. Kaneda and K. Suga*
Department of Mechanical Engineering,
Osaka Prefecture University
1-1 Gakuen-cho, Naka-ku, Sakai, Osaka 599-8531, Japan
*email: suga@me.osakafu-u.ac.jp

ABSTRACT

PIV measurements have been performed for turbulent flows in a rib-mounted channel whose bottom wall is made of a porous layer. The effects of the wall and rib permeability are investigated focusing on the separating and reattaching flows. Three kinds of porous media are employed. They have the same porosity of 0.8 but each permeability is different from the others. Two kinds of square cylinder ribs: an impermeable smooth solid rib or a permeable porous rib which is made of the same porous medium as that for the bottom wall are used. The obtained mean velocity profiles of the solid rib flows suggest that the reverse flow in the recirculation behind the rib becomes weak as the increase of the wall permeability. The main factor is found to be the increase of the by-pass flow rate through the bottom porous wall underneath the solid rib. Due to the reduction of the magnitude and the size of the reverse flow region in the clear channel, turbulence becomes weaker than that of the solid-rib mounted solid-wall channel flow. However, because of the entrainment flow to the shear layer through the porous wall, the near wall turbulent intensities are enhanced. In the porous rib flow, the recirculation and the reattachment point shift downstream further. As the increase of the permeability, the recirculation is finally vanished. These are due to the flows not only through the bottom wall but also through the rib. Because of the flow through the porous rib, which weakens the shear layer behind the rib, turbulence become weaker than that of the solid-rib flows. In both the solid and porous rib flows, it is confirmed that a reverse flow region exists inside the porous wall whereas the reverse flow is not obvious in the clear channel region at a higher Reynolds number and/or higher permeability.

INTRODUCTION

Flow physics around a highly porous material is of great interest in designing flow passages of industrial devices such as those in catalytic converters. Due to the wall permeability, turbulent eddy vortex motions over porous walls are not damped so much as near solid walls resulting in strong near-wall shear stress production. (The detailed PIV measurement to investigate such phenomena in a turbulent channel was reported by the present authors recently: Suga et al., 2010; 2011.) It is then understandable that if the flow includes separation near a porous wall, the formation of a separation bubble is strongly affected by the wall permeability. Thus, in our previous study (Suga et al., 2009), the difference between the phenomena over rib-mounted permeable and impermeable walls was preliminary discussed based on PIV experiments. The results indicated that over a porous wall the separation bubble behind the rib became smaller at higher Reynolds numbers due to the increase of the by-pass flow rate through the porous wall under the rib. However, since only a single kind of porous medium was applied, the effects of the wall permeability were not clear in the previous study. Therefore, in the present study, to complete the discussion of the effects of the wall permeability on the turbulence characteristics in separating flows over permeable porous materials, further PIV measurements of two velocity components of the turbulent fields over rib-mounted porous walls are carefully performed. Three kinds of foamed ceramics are used as the porous media. All of them have the same porosity of φ =0.8 but the permeability varies as K= 0.020-0.087 mm^2 as listed in Table 1.

Table 1. Characteristics of the porous media.

Porous med. No.	φ	K [mm^2]	D_p [mm]
#20	0.82	0.020	1.7
#13	0.81	0.033	2.8
#06	0.80	0.087	3.8

EXPERIMENTAL METHOD

Fig.1 illustrates the present experimental flow geometry where one of the channel walls is a solid smooth acrylic wall

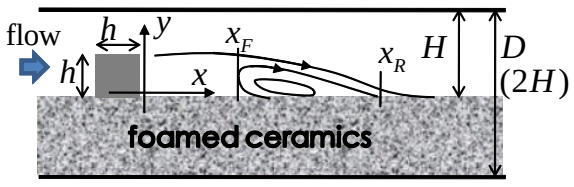

Figure 1. Flow field geometry.

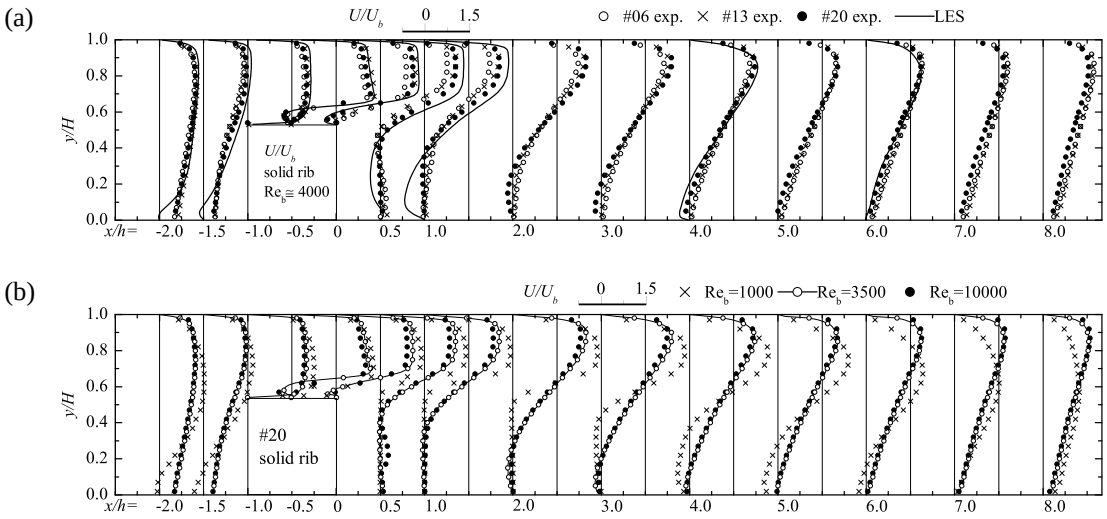

Figure 2. Mean streamwise velocity profiles in the solid rib flows; (a) effects of the wall permeability at $\mathrm{Re}_b \simeq 4000$, (b) effects of Re_b in case #20.

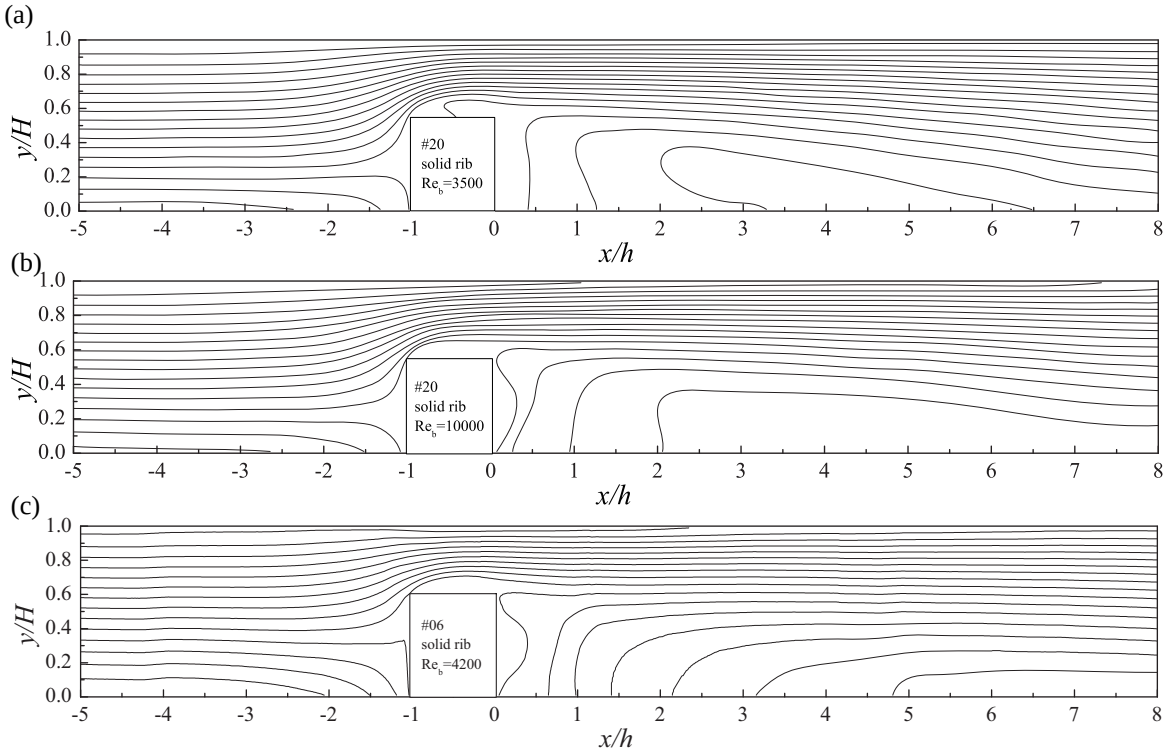

Figure 3. Streamlines of the solid rib flows; (a) case #20 at Re_b =3500, (b) case #20 at Re_b =11500 (c) case #06 at Re_b=4200.

(top wall) whilst the other (bottom wall) is made of a porous medium (foamed ceramics) whose porosity φ, permeability K and mean pore diameter D_P are listed in Table 1. The thickness of the porous wall is 0.03 m which is the same as the height H of the clear fluid channel region whose width is 0.3 m. Hence, the flow is nominally two-dimensional near the symmetry plane of the channel. (This is also confirmed by the measurements.) In the test section, a square sectioned rib whose height is $h(=H/2)$ is mounted as shown in Fig.1. Upstream the test-section, the channel length is 3.0 m to make the flow fully developed. The working fluid is tap water and acrylic colloid particles whose mean diameter is 3 μ m are used for the tracer particles of the PIV measurement. The measured range of the bulk Reynolds number Re_b ($\rho U_b H/\mu$) is 1000-10000 where the viscosity μ and the density ρ are estimated using the measured water temperature. The bulk mean velocity U_b is obtained by integrating the measured sectional mean velocity profile at $x=-5h$ where the flow is unaffected by the rib.

The present two-component PIV system consists of a double-pulse Nd-YAG laser with 120 mJ/pulse at a frequency of 532 nm, a CCD camera of 30 fps, a camera lens of 60

Table 2. Characteristics of recirculation bubbles and by-pass flow rates.

rib	case	Re_b	x_F/h	x_R/h	$\frac{Q_p\|_{x=-h}}{Q_b}$
solid	#20	1050	0	6.7	0.09
		3500	0	5.2	0.14
		10200	0	5.4	0.17
	#13	1150	0	7.0	0.16
		3600	–	–	0.22
		9900	–	–	0.26
	#06	1150	0	4.8	0.24
		4200	–	–	0.24
		11500	–	–	0.25
porous	#20	1000	–	9.0	0.21
		3450	3.8	8.5	0.31
		9750	6.1	10.0	0.34
	#13	1250	–	–	0.37
		3900	–	–	0.40
		9900	–	–	0.43
	#06	1000	–	–	0.43
		4000	–	–	0.43
		10000	–	–	0.43

mm f/2.8 and a computer for data acquisition. The laser beam is formed into a sheet of approximately 1.0 mm thickness through several cylindrical lenses. The sheet illuminates the symmetry plane of the channel where the instantaneous images are recorded by the CCD camera. A single recorded frame covers a zone of 30×30 mm^2 with 2048×2048 pixels. To cover the measurement area of $-5h \le x \le 8h$, 8 zones, which have overlapping areas of approximately $0.175H$ with the neighbour zones, are measured. The number of the particle is adjusted to be about 10 in an interrogation window whose size is set to 32×32 pixels. The uncertainty in the measured displacement can be expected to be roughly less than 1/20 of the diameter of the particle image. Normalising the uncertainty of this mean displacement of particles yields a relative error of less than 4%. To obtain the statistical data, in each zone, 4800 image pairs are processed in this study.

RESULTS AND DISCUSSIONS

Solid Rib Flows

Fig.2 show examples of the mean streamwise velocity U profiles obtained. In Fig.2(a), the LES data are from Abe & Suga (2001) and correspond to a solid wall flow in which the wall permeability is zero. As listed in Table 1, as the porous medium number decreases from #20 to #06, the permeability increases from 0.020 to 0.087 mm^2. Thus, as the wall permeability increases, it is recognisable that the reverse flow region in the clear channel tends to shrink. As in Fig.2(b), although case #20 at Re_b=1000 where the inlet flow is laminar shows different flow profiles, the profiles by fully turbulent inlets at $\mathrm{Re}_b \ge 3500$ look very similar to each other.

In order to see the averaged flow patterns, by calculating the stream functions using the measured mean velocities, Fig.3 compares the streamlines of the solid rib flows over different porous-walls. Figs.3(a) and (b) compare the effects of the bulk Reynolds number, Re_b in case #20 whilst Figs.3(a) and (c) compare the effects of the wall permeability at $\mathrm{Re}_b \simeq 4000$. When the Re_b increases, it is recognisable that the reverse flow region in the clear channel tends to vanish (Figs.3(a) and (b)). Also, as shown in Fig.3 (c), due to the increase of the permeability of the porous wall (as shown in Table 1, case #06 is about 4.5 times more permeable than case #20), the recirculation bubble in the clear channel is weakened and nearly extinguished. This is because more amount of the flow upstream the rib goes inside the bottom wall layer and bleeds out behind the rib as the permeability increases. Table 2 summarises the locations of the front edge and reattachment point of the recirculation bubble, which are respectively denoted by x_F and x_R. Since in cases #13 and #06 at $\mathrm{Re}_b > 3500$, the recirculation bubble cannot be detected, no information is given in the table. It is recognised that at a higher Re_b and higher permeability, the recirculation bubble generally tends to shrink and vanish.

The by-pass flow phenomenon can be confirmed in Fig.4 where the distribution of the sectional flow rate: $Q_c = \rho \int_0^H U dy$,is compared. (The bulk flow rate Q_b is $Q_c|_{x=-5h}$.) At the location where the difference: $(Q_c - Q_b)$ is negative, such an amount of fluid goes through the porous wall. The entrainment flow for the development of the shear layer behind the rib is partly supplied by this by-pass flow. Although the by-pass flow rate increases as the increase of the permeability as in Fig.4, the more interesting effect is observed in the entrainment flow from the downstream region. As the increase of the wall permeability from #20, it is clearly seen that the normalized flow rate increases and further exceeds 1.0 in the region $x/h > 3$. This implies that the entrainment from further downstream region increases and a reverse flow region does exist inside the porous wall whereas the reverse flow is not obvious in the clear channel region. Thus, as the increase of the wall permeability, it is assumed that the recirculation bubble tends to submerge inside the porous wall and the reverse flow inside the wall becomes stronger. (The difference between cases #13 and #06 is marginal at $x/h > 2$ and the effect looks saturated. This may imply that the flow is affected by the finite thickness of the porous layer in the higher permeability case. However, it is confirmed that case #20 is unaffected by the layer thickness by measuring the flow over a porous layer of a half thickness.) At the higher Re_b case, because of the larger pressure difference between the upstream and the downstream of the rib, a larger amount of the flow by-passes

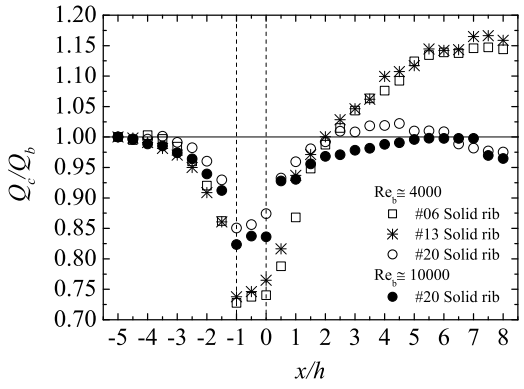

Figure 4. Normalized flow rates in the solid rib flows.

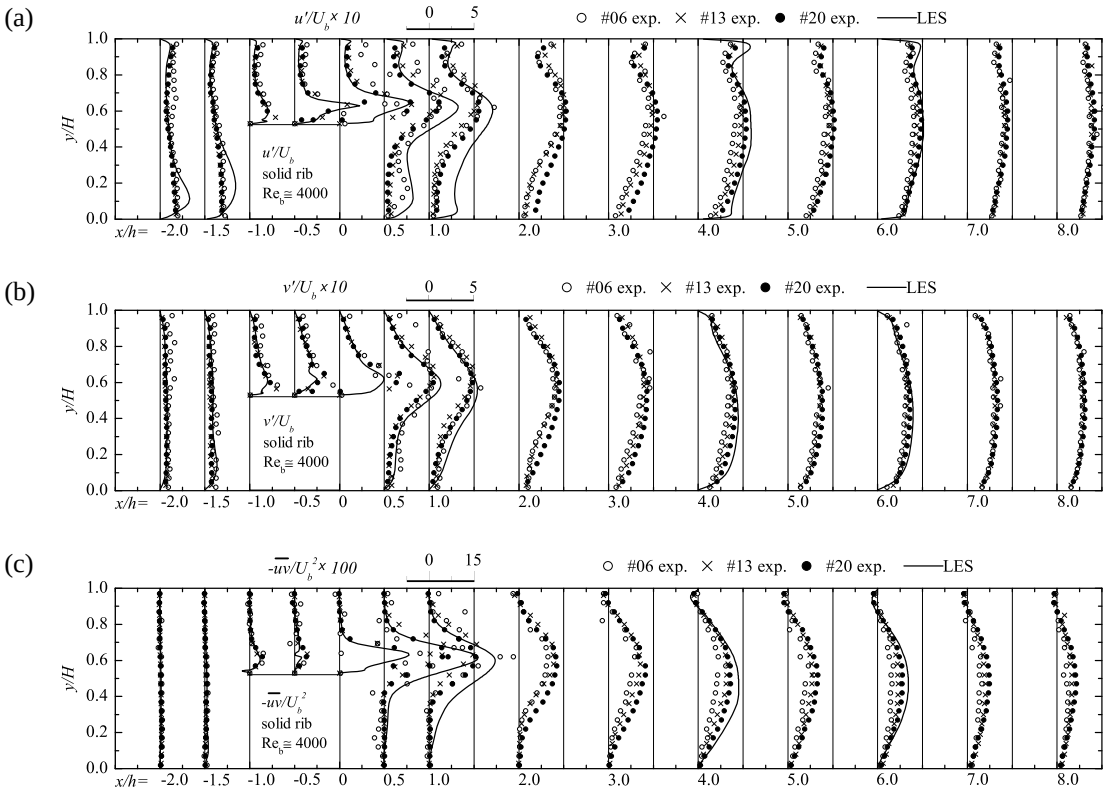

Figure 5. Turbulent intensities and the Reynolds shear stress profiles in the solid rib flows at $Re_b \simeq 4000$; (a) streamwise turbulent intensity, (b) wall-normal turbulent intensity, (c) Reynolds shear stress.

through the bottom wall layer resulting in reducing more the size of the recirculation bubble behind the rib (Fig.3(b)). Table 2 also summarises the by-pass flow rate $Q_p = Q_b - Q_c$ at the location of the upstream rib-face: $x = -h$. It is obvious that the by-pass flow rate increases as the increase of Re_b and the wall permeability.

Fig.5 compares the turbulent intensities u', v' and the Reynolds shear stress $-\overline{uv}$ profiles at $Re_b \simeq 4000$. Although the level of turbulence is very high behind the rib compared with those in the inlet region, it tends to be lower as the wall permeability increases. The shear layer behind the rib tends to be weakened due to the weakened reverse flow and this causes the reduction of the shear stress production. Thus, the turbulent intensities have generally the same tendency as that of the Reynolds shear stress. However, the wall normal component v' shows an interesting tendency near the wall. As shown in Fig.6(b), the near wall value of v' increases as the wall permeability increases clearly in the region $1.0 < x/h < 2.0$. This indicates that due to the increase of the wall permeability, wall normal vortex motions are enhanced near the wall and penetrate deeper inside the porous wall. When the near-wall distributions of u' and v' are compared (Figs.6(a) and (b)), it is noticeable that at the highest permeability case, case #06, the level of v' is clearly larger than that of u' very near the wall in the region of $1.0 < x/h < 2.0$. This is partly because the mean flow direction there is perpendicular to the wall as indicated in Fig.3(c). As the increase of the wall permeability, the bleeding flow rate from underneath the wall is enhanced and the flow is entrained straightly to the shear layer behind the rib. This is also supported by the increase of the gradient of the flow rate behind the rib as the wall permeability increases which is shown in Fig.4.

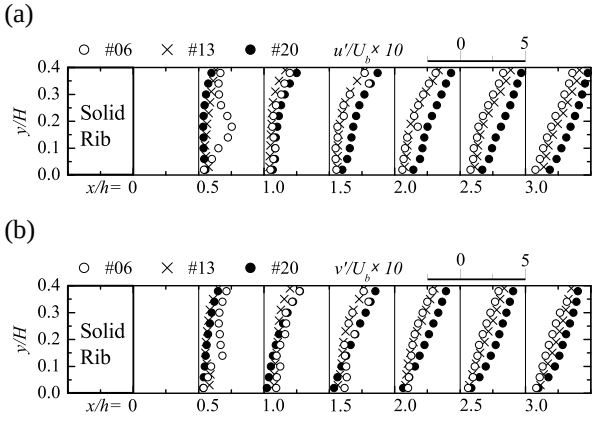

Figure 6. Near-wall comparison of turbulent intensities at $Re_b \simeq 4000$; (a) streamwise turbulent intensity, (b) wall-normal turbulent intensity.

Porous Rib Flows

When the rib has permeability, since the flow also goes through the rib, the flow pattern and turbulence quantities change. Figs.7(a)-(e) show streamlines and turbulence quantities in the porous rib flows of #20 at $Re_b \simeq 4000$. Due to the flow going through the rib, as shown in Fig.7(a), the recirculation zone shifts downstream compared with the solid

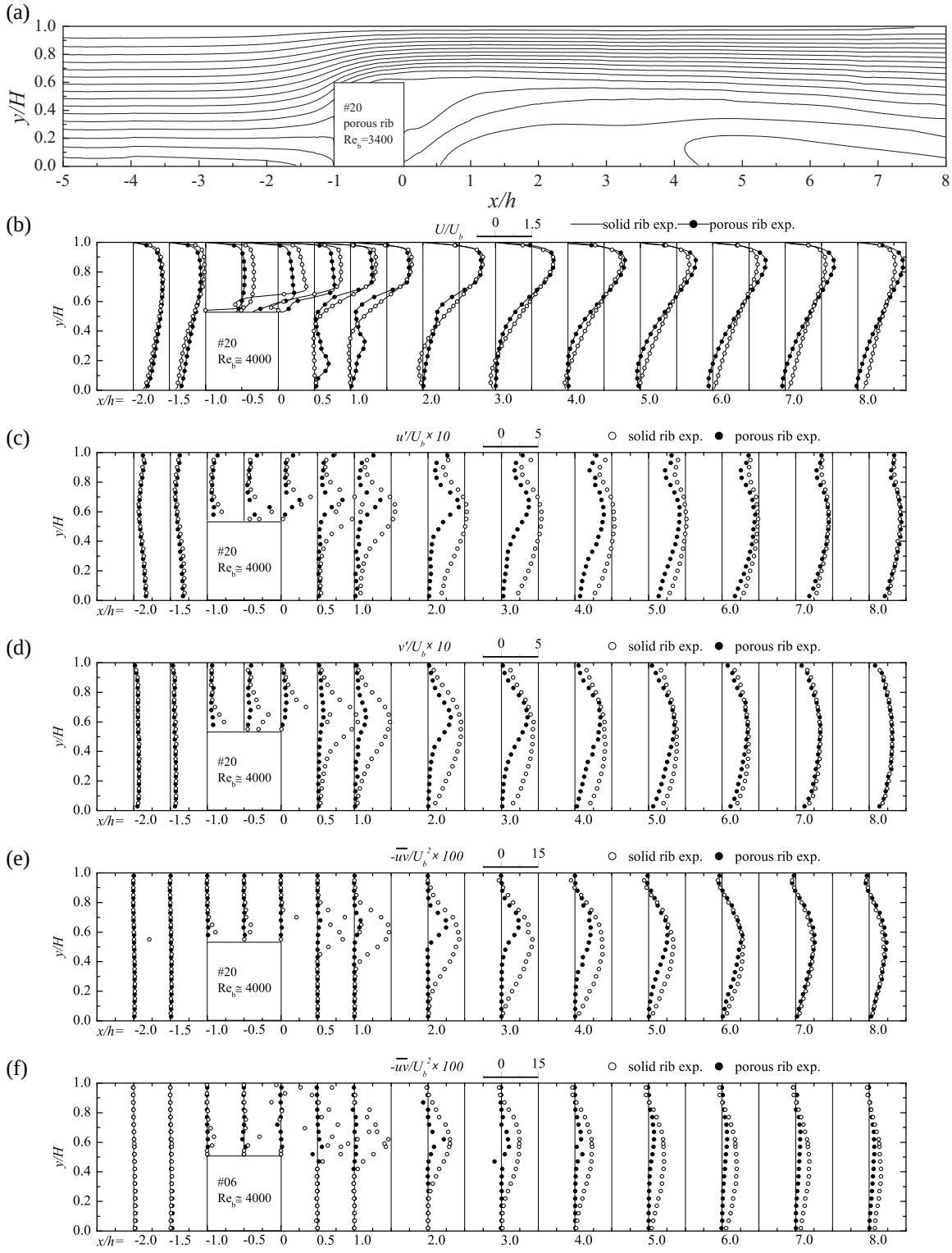

Figure 7. Streamlines in the porous rib flow of #20 and comparison of the turbulent flow quantities between porous and solid rib flows at $\mathrm{Re}_b \simeq 4000$; (a) streamlines of the porous rib flow (b) mean streamwise velocity (#20), (c) streamwise turbulent intensity (#20), (d) wall-normal turbulent intensity (#20), (e) Reynolds shear stress (#20), (f) Reynolds shear stress (#06).

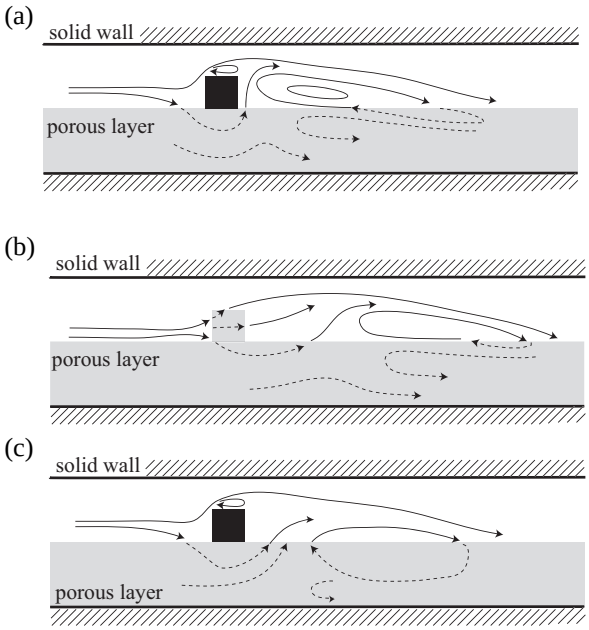

Figure 8. Flow patterns confirmed by the experiments; (a) solid rib flow, (b) porous rib flow, (c) solid rib flow at a higher Re_b and/or wall permeability.

rib flow of Fig.3(a). Indeed, in Fig.7(b), it is clear that the streamwise velocity U becomes larger behind the rib and the negative flow region appears in a further downstream region than in the solid rib flow. As the increase of the permeability, however, the reverse flow becomes weaker and the recirculation zone tends to vanish. Such a tendency is obvious in the variation of x_F and x_R listed in Table 2. As shown in Table 2, the normalized by-pass flow rate $(Q_p|_{x=-h})/Q_b$ increases as the increase of Re_b and/or the permeability. (In the porous rib flows, the by-pass flow rate defined at $x=-h$ includes the flow going through the rib.) This tendency is the same as in the solid rib flows whilst the normalised by-pass flow rate tends to saturate to the value of 0.43.

The distribution of turbulent intensities u',v' and the Reynolds shear stress $-\overline{uv}$ profiles shown in Figs.7(c)-(e) indicate that the turbulence is weakened in the region of $-1 < x/h < 6$ in the porous rib flow. This is because the reverse flow behind the rib is weakened and thus the shear layer comes loose. In the further downstream region of $7 < x/h$ the turbulence recovers to the same level as in the solid rib flow, whilst the turbulence never catches up in the higher permeability cases of #13 and #06 as in Fig.7(f).

Flow Patterns

Fig.8 illustrates the flow patterns confirmed by the present experiments. As in Fig.8(a), in the solid rib flows, a part of the flow goes into the porous bottom layer due to the blocking by the rib and bleeds out in the region behind the rib contributing to the entrainment to the developing shear layer formed from the front edge of the rib. Because of the wall permeability, a part of the recirculation bubble submerges into the bottom layer. As in Fig.8(b), when the rib has permeability, the recirculation bubble shifts downstream due to the effects of the flow passing through the rib. In cases at a higher Re_b and/or wall permeability, the recirculation bubble submerges further and thus the reverse flow region in the clear channel vanishes as in Fig.8(c). It is confirmed that both the solid and porous rib flows share this tendency.

CONCLUDING REMARKS

The results indicate that a turbulent recirculation or wake flow region is formed behind the rib in all the flow cases measured at $10^3 \leq \mathrm{Re}_b \leq 10^4$. However, since a part of entraining fluid is supplied through the permeable bottom wall from the region upstream the rib, the magnitude of the reverse flow of the recirculation in the clear channel becomes lower as the increase of the wall permeability. The separation bubble in the solid-rib flow thus is smaller and its reattachment length becomes shorter as the increase of the wall permeability and/or the Reynolds number. Due to the reduction of the magnitude and the size of the reverse flow region in the clear channel, turbulent intensities and the Reynolds shear stress become smaller than those of the solid-rib mounted solid-wall channel flow. However, due to the entrainment flow to the shear layer through the porous wall, the near wall turbulent intensities are enhanced. Particularly, the wall normal component tends to be larger as the wall permeability increases.

In the porous-rib flows (the rib material is the same as that of the porous wall), because of the fluid passing through the rib, the recirculation is more significantly weakened and shifts downstream. The upstream edge of the recirculation shifts further downstream as the increase of the Reynolds number in case of #20 whereas no recirculation region is observed in the clear channel at the higher wall permeability regardless of the Reynolds number measured. Due to the reduced pressure drop by the permeability of the rib, the flow rate through the bottom wall becomes smaller than that of the solid rib flow. Because of the flow through the porous rib, turbulent intensities and the Reynolds shear stress become smaller than those of the solid-rib flows.

In both the solid and porous rib flows, since the entrainment flow from the downstream region generally increases as the wall permeability increases, a reverse flow region does exist inside the porous wall whereas the reverse flow is not obvious in the clear channel region. Therefore, as the increase of the wall permeability, it is confirmed that the recirculation bubble tends to submerge inside the porous wall layer.

REFERENCES

Abe, K. and Suga, K., 2001, "Large eddy simulation of passive scalar in complex turbulence with flow impingement and flow separation", Heat Transfer Asian Res, Vol.30, pp.402–418.

Suga, K., Matsumura, Y., Tominaga, S., Ashitaka, Y., Kaneda, S., 2010, "Effects of wall permeability on turbulence", Int. J. Heat Fluid Flow, Vol.31, pp. 974–984.

Suga, K., Mori, M., Kaneda, S., 2011, "Vortex structure of turbulence over permeable walls", Int. J. Heat Fluid Flow, Vol.32, in press.

Suga, K., Tominaga, S., Kaneda, M., 2009, "An experimental study on turbulence over rib-mounted permeable walls", Proc. Turbulence, Heat and Mass Transfer 6, CD-ROM, Rome, Italy.